

Kinetics of Formation for *n*-Alkanethiolate Self-Assembled Monolayers onto Gold in Aqueous Micellar Solutions of C₁₂E₆ and C₁₂E₇

Dong Yan, Jeremy A. Saunders, and G. Kane Jennings*

Department of Chemical Engineering, Vanderbilt University, Nashville, Tennessee 37235

Received April 30, 2002. In Final Form: September 16, 2002

We have investigated the kinetics of formation for *n*-alkanethiolate self-assembled monolayers (SAMs) onto gold from aqueous micellar solutions of hexaethylene glycol monododecyl ether (C₁₂E₆) and heptaethylene glycol monododecyl ether (C₁₂E₇). Micelles provide hydrophobic domains to solubilize the alkanethiols in aqueous solution and facilitate their delivery to the gold surface. The kinetics of SAM formation depends on the micellar size, the concentration of solubilized thiol, and the alkanethiol chain length. The kinetics data for SAM formation in aqueous micellar solutions of C₁₂E₆ and C₁₂E₇ are best fit by a diffusion-limited, second-order Langmuir adsorption model that accounts for diffusion of the thiol-laden micelles and release of the alkanethiols from the micelles. The observed rate constant for SAM formation decreases exponentially with alkanethiol chain length, consistent with an activated diffusion process for the release of the alkanethiol from the micelle. The activation energy for release of the thiols from the C₁₂E₆ and C₁₂E₇ micelles to the metal surface is ~0.22 kcal/mol per CH₂ group in the alkanethiol. This relatively small barrier is consistent with a mechanism in which alkanethiols release from micelles to admicelles that are present on the gold surface through a collision-induced process.

Introduction

Self-assembled monolayers (SAMs)¹ formed by the adsorption of alkanethiols onto various metal surfaces enable the generation of densely packed molecular barrier films for potential applications in lithography,² molecular capacitors,³ and corrosion inhibition.^{4,5} In these applications, the ability to form high-quality SAMs with minimal defect densities can be crucial. In addition, as the applications of SAMs extend into commercial development, the engineering of affordable, effective, and environmentally benign methods to form these films with high throughput will be required.

We have recently used aqueous micellar solutions of hexaethylene glycol monododecyl ether (C₁₂E₆) as solvent for the preparation of *n*-alkanethiolate SAMs on gold.⁶ In this micelle-assisted formation process, long-chain alkanethiols that are insoluble in water are solubilized within the hydrophobic cores of the micelles and delivered to the metal surface. The resulting SAMs exhibit greater overall chain density and improved barrier properties in comparison to SAMs formed from ethanol and hydrocarbon solvents.⁶ We have attributed these superior properties to the effect of hydrophobic interactions between the alkyl chains of the assembling thiolates in the aqueous environment that promote the formation of SAMs with large domains and few defects. The micelle-assisted formation

of SAMs therefore represents an environmentally benign process to prepare films of extremely high quality.

In this paper, we extend our efforts to investigate the kinetics of SAM formation from aqueous micellar solutions of hexaethylene glycol monododecyl ether (C₁₂E₆) and heptaethylene glycol monododecyl ether (C₁₂E₇). For the application of micellar delivery vehicles to form SAMs, these nonionic surfactants offer numerous advantages, including a low critical micelle concentration (cmc), environmental biodegradability, and controllable aggregation numbers (*N*_{agg}), depending on the number of ethylene oxide units (*j*) (Table 1) and temperature.^{7–9} This last fact is illustrated in Table 1 where C₁₂E₇ forms spherical micelles with lower aggregation numbers and C₁₂E₆ forms a more polydisperse mixture of spherical and cylindrical micelles at room temperature and exhibits a higher average aggregation number.

A detailed study of the kinetics of formation for these water-borne SAMs is important to understand the complex film formation dynamics and establish a protocol for the fabrication of reproducible, densely packed, and complete monolayers with minimal defects. The kinetics of formation for SAMs in organic solvents has been studied by a variety of techniques such as ellipsometry,¹⁰ second harmonic generation (SHG),¹¹ quartz crystal microbalance,¹² surface plasmon resonance spectroscopy,¹³ and scanning

* To whom correspondence should be addressed. E-mail: jenningsk@vuse.vanderbilt.edu.

(1) *Thin Films*; Ulman, A., Ed.; Academic Press: Boston, MA, 1998; Vol. 24.

(2) Kumar, A.; Biebuyck, H. A.; Whitesides, G. M. *Langmuir* **1994**, *10*, 1498–1511.

(3) Haag, R.; Rampi, M. A.; Holmlin, R. E.; Whitesides, G. M. *J. Am. Chem. Soc.* **1999**, *121*, 7895–7906.

(4) Laibinis, P. E.; Whitesides, G. M. *J. Am. Chem. Soc.* **1992**, *114*, 9022–9027.

(5) Jennings, G. K.; Munro, J. C.; Yong, T.-H.; Laibinis, P. E. *Langmuir* **1998**, *14*, 6130–6139.

(6) Yan, D.; Saunders, J. A.; Jennings, G. K. *Langmuir* **2000**, *16*, 7562–7565.

(7) Mukerjee, P.; Mysels, K. J. In *Critical Micelle Concentrations of Aqueous Surfactant Systems*; U.S. Department of Commerce: Washington, D.C., 1971; Vol. 36.

(8) Brown, W.; Johnsen, R.; Stilbs, P.; Lindman, B. *J. Phys. Chem.* **1983**, *87*, 4548–4553.

(9) Brown, W.; Zhou, P.; Rymden, R. *J. Phys. Chem.* **1988**, *92*, 6086–6094.

(10) Bain, C. D.; Troughton, E. B.; Tao, Y.-T.; Evall, J.; Whitesides, G. M.; Nuzzo, R. G. *J. Am. Chem. Soc.* **1989**, *111*, 321–335.

(11) Dannenberger, O.; Buck, M.; Grunze, M. *J. Phys. Chem. B* **1999**, *103*, 2202–2213.

(12) Karpovich, D. S.; Blanchard, G. J. *Langmuir* **1994**, *10*, 3315–3322.

(13) Peterlinz, K. A.; Georgiadis, R. *Langmuir* **1996**, *12*, 4731–4740.

Table 1. Surfactants Studied

surfactant	composition	cmc (mM) ⁷	micelle structure	$N_{\text{agg}}^{25^\circ\text{C}}$
C ₁₂ E ₆	CH ₃ (₂) ₁₁ (OCH ₂ CH ₂) ₆ OH	0.087 ²⁰ °C	cylindrical/spherical	310 ⁸
C ₁₂ E ₇	CH ₃ (₂) ₁₁ (OCH ₂ CH ₂) ₇ OH	0.075 ²³ °C	spherical	140 ⁹

probe microscopy.^{14,15} These techniques have led to an improved understanding of how alkanethiol-based SAMs form in organic solvents. In situ microscopy studies^{14,15} have illustrated that these SAMs are formed through the following multistep process: (1) physically adsorbed alkanethiols that are lying flat on the surface chemisorb to produce oriented alkanethiolates; (2) these oriented alkanethiolates nucleate to form well-ordered, densely packed islands or domains that spread across the surface with time as additional alkanethiols adsorb at the domain boundaries; (3) at high coverages, these growing domains merge with other domains to form a nearly complete film with few defects. Dannenberger et al.¹¹ have used SHG to study the effects of solvent and chain length on the kinetics of formation for *n*-alkanethiolate SAMs onto gold. Their work demonstrates that the formation of SAMs from a variety of alkane solvents and ethanol can be approximated by a first-order Langmuir adsorption process in which the displacement of adsorbed solvent molecules and/or the incorporation of alkanethiols into growing domains of thiolates are the rate-limiting steps. Solvents that interact strongly with alkanethiols or with the gold surface can significantly impede the kinetic rate of SAM formation.¹¹

Liu and Kaifer¹⁶ reported the preparation of alkanethiolate SAMs onto gold using aqueous micellar solutions of Triton X-100, sodium dodecyl sulfate, and hexadecyltrimethylammonium bromide as solvents. They used ex situ electrochemical measurements to determine that the kinetics of C₁₂S- SAM formation depends on the concentration of surfactant at constant thiol concentration. Below the cmc, the SAM does not form, but above the cmc, the kinetic rate for SAM formation increases with surfactant concentration as the higher concentration of micelles enhances the solubilization of the thiol adsorbates. As surfactant concentration is increased further, the rate decreases, presumably due to a larger fraction of "empty" micelles. To our knowledge, there has been no report on the in situ kinetics of SAM formation in aqueous micellar solutions.

The micelle-assisted formation of alkanethiolate SAMs likely involves several steps including solubilization of the alkanethiols in the micellar cores, diffusion of the thiol-laden micelles near the surface, release of the alkanethiols from the micelle, and displacement of adsorbed surfactant and water by the alkanethiols prior to adsorption. Of particular importance is how the alkanethiols are released from the micelles, whether into water, to surface micelles, or directly onto the gold surface. Jaschke et al.¹⁷ have characterized the surface micelles or admicelles formed on gold surfaces upon exposure to aqueous solutions containing various surfactants above their cmc. In the absence of ion templating effects, the admicelles consist of long, hemicylindrical structures that are stable to imaging by in situ atomic force microscopy (AFM). Admicelles have been used to solubilize various organic molecules onto high-surface-area solids such as alumina

particles and porous silica.^{18–20} These adsolubilization studies have focused primarily on equilibrium conditions with solute molecules that are marginally to completely water soluble and have no chemical attraction for the surface. The present system is more dynamic, since the water-insoluble alkanethiols displace admicelles and chemisorb to the surface over time. Through in situ characterization of the kinetics of SAM formation in aqueous micellar solutions, we seek to uncover mechanistic aspects of the delivery, release, and adsorption processes.

The major advantage to studying the kinetics of SAM formation in aqueous solution is that electrochemical techniques can be utilized to monitor the assembly process in situ. To characterize micelle-assisted SAM formation in situ, we have modified an impedance method developed by Subramanian and Lakshminarayanan,²¹ who studied the kinetics of SAM formation in ethanol. In situ impedance measurements are extremely useful for studying the early stages of SAM formation, when capacitance changes are most sensitive to the growth of the monolayer film. By monitoring the kinetics of micelle-assisted SAM formation in situ, we can gain fundamental insight on the mechanistic aspects of film growth, including the effects of alkanethiol chain length and concentration and surfactant/micelle composition on the assembly process. Therefore, in a broader sense, the micelle-assisted formation of SAMs represents a model system that can provide mechanistic information to impact various micellar delivery and release processes including adsolubilization and micellar drug delivery.^{22–24} For example, studying the effects of alkanethiol chain length and concentration on the kinetic rates of SAM formation may provide useful parallels to the effects of drug hydrophobicity and concentration in more complex in vivo systems that are difficult to characterize.

Results

Solubilization of Alkanethiols in Micellar Solutions. We have used ¹H NMR to determine the solubility of various *n*-alkanethiols in 10 mM solutions of C₁₂E₆(aq) and C₁₂E₇(aq). Since the cmc for each of these surfactants is <0.1 mM, the concentration of 10 mM represents the approximate concentration of surfactants that are in micelles. Table 2 displays the concentrations of solubilized alkanethiols in the micelles when enough thiol is added to form a 1 mM solution, a typical concentration used to study the formation of SAMs. Values less than 1.0 indicate that all the added thiol is not solubilized. As shown in Table 2, C₁₀SH and C₁₂SH are both solubilized at 1 mM in 10 mM C₁₂E₆(aq) and C₁₂E₇(aq), but C₁₆SH and C₁₈SH are solubilized more effectively in C₁₂E₆(aq). These results

(18) Lee, C.; Yeskie, M. A.; Harwell, J. H.; O'Rear, E. A. *Langmuir* **1990**, *6*, 1758–1762.

(19) Monticone, V.; Treiner, C. *Langmuir* **1995**, *11*, 1753–1758.

(20) Saeki, A.; Sakai, H.; Kamogawa, K.; Kondo, Y.; Yoshino, N.; Uchiyama, H.; Harwell, J. H.; Abe, M. *Langmuir* **2000**, *16*, 9991–9995.

(21) Subramanian, R.; Lakshminarayanan, V. *Electrochim. Acta* **2000**, *45*, 4501–4509.

(22) Harada, A.; Kataoka, K. *Macromolecules* **1995**, *28*, 5294–5299.

(23) Scholz, C.; Iijima, M.; Nagasaki, Y.; Kataoka, K. *Macromolecules* **1995**, *28*, 7295–7297.

(24) Kwon, G. S.; Kataoka, K. *Adv. Drug Delivery Rev.* **1995**, *16*, 295–309.

(14) Yamada, R.; Uosaki, K. *Langmuir* **1998**, *14*, 855–861.

(15) Xu, S.; Cruchon-Dupeyrat, S.; Garno, J. C.; Liu, G.-Y.; Jennings, G. K.; Yong, T.-H.; Laibinis, P. E. *J. Chem. Phys.* **1998**, *108*, 5002–5012.

(16) Liu, J.; Kaifer, A. E. *Isr. J. Chem.* **1997**, *37*, 235–239.

(17) Jaschke, M.; Butt, H.-J.; Gaub, H. E.; Manne, S. *Langmuir* **1997**, *13*, 1381–1384.

Table 2. ¹H-NMR-Determined Alkanethiol Concentration (mM) in 10 mM C₁₂E₆ and C₁₂E₇(aq)^a

surfactant	C ₁₀ SH	C ₁₂ SH	C ₁₆ SH	C ₁₈ SH
C ₁₂ E ₆	1.0	1.0	1.0	0.25
C ₁₂ E ₇	1.0	1.0	0.30	0.15

^a Enough thiol is added to form 1 mM solution if all the thiol is solubilized.

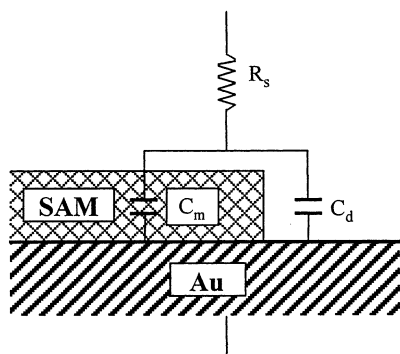


Figure 1. Schematic of a parallel capacitance model used to relate interfacial capacitance to film coverage. R_s = solution resistance, C_m = capacitance of thiolate domains (per unit area), C_d = capacitance of the gold surface exposed to the aqueous surfactant solution (per unit area).

are consistent with previous studies,²⁵ which conclude the solubilizing power of the micelles increases with aggregation number (C₁₂E₆ > C₁₂E₇). The longer chain length alkanethiols are less soluble than shorter ones in micellar solutions due to the larger molecular volume required for solubilization. These hydrophobic alkanethiol molecules are likely solubilized in the core of the micelles. Honda et al.²⁶ have used fluorescence spectra to show that pyrene molecules reside mainly in the core region of C₁₂E₇ ($i = 10, 12, 14$, and 16) micelles. Since long-chain alkanethiols are generally more hydrophobic than pyrene,²⁷ we expect the alkyl tail of the alkanethiols to reside predominantly in the micellar core.

In Situ Monitoring of Kinetics. We have used interfacial capacitance measurements to assess the in situ kinetics of SAM formation from aqueous micellar solutions. As shown by in situ AFM, the growth of a SAM can be described by the formation, growth, and ultimately, the coalescence of islands or domains that contain alkanethiolates in an ordered ($\sqrt{3} \times \sqrt{3}$)R30° lattice.¹⁵ As the coverage of the monolayer increases by the growth of these domains, additional adsorbed thiolates block sites on the gold surface, reducing the interfacial capacitance. To relate capacitance to coverage, we assume the substrate–solution interface is composed of two parts in parallel (Figure 1). One part consists of adsorbed alkanethiolates with coverage $\theta(t)$ where the film capacitance is C_m (all capacitances are per unit area), and the other part is the gold surface that is uncoated by thiol molecules and has a capacitance of C_d . Here, C_d represents the interfacial capacitance before the thiol molecules are introduced and is affected by the double layer capacitance and preadsorbed surfactant molecules or admicelles, consistent with those characterized by Jaschke et al.¹⁷ While C_d and C_m are

assumed constant and are measured at the beginning and end of the experiment, respectively, $\theta(t)$ changes from 0 at $t = 0$ to 1.0 after the monolayer has completely formed. The interfacial capacitance ($C(t)$) is thus written as a linear combination of C_m and C_d :

$$C(t) = C_m \theta(t) + C_d (1 - \theta(t)) \quad (1)$$

The capacitance can be related to the impedance modulus and phase angle by²⁸

$$C(t) = -\frac{1}{2\pi f Z(t) \sin \Phi(t)} \quad (2)$$

where f is the frequency (100 Hz), $Z(t)$ is the impedance modulus, and $\Phi(t)$ is the phase angle. The transient coverage can then be calculated by combining eqs 1 and 2 as

$$\theta(t) = \frac{C_d + \frac{1}{2\pi f Z(t) \sin \Phi(t)}}{C_d - C_m} \quad (3)$$

providing real time feedback on the extent of monolayer formation by simply monitoring the impedance modulus and phase angle. The interfacial capacitance is very sensitive to the initial, fast adsorption of alkanethiols and becomes relatively constant during the film ordering, as few available sites remain on the surface and the dielectric properties of the film change more subtly with time.

The use of eq 3 to monitor kinetics in situ relies on a few assumptions regarding the nature of the assembly process. As discussed above, and inherent to eq 1, the forming SAM is assumed to consist of domains that grow with time, displacing adsorbed micelles from the surface. These domains are known to be well ordered, exhibiting a ($\sqrt{3} \times \sqrt{3}$)R30° lattice¹⁵ and should exhibit capacitances per unit area that are nearly constant during growth. We assume that the presence of physisorbed thiols that lie parallel to the gold surface or exist within surface micelles does not significantly alter the interfacial capacitance from that of the preadsorbed surface micelles. In other words, we assume that the measured changes in capacitance upon thiol addition are due primarily to the formation and growth of densely packed chemisorbed thiolate domains that electrochemically block the gold surface from the aqueous solution.

To investigate the assembly process in more detail, we exposed a gold surface initially in an aqueous solution containing 50 mM NaF,²⁹ which was added to increase the ionic strength for these electrochemical measurements, to a step change in concentration of C₁₂E₆ from 0 to 10 mM while keeping the concentration of NaF constant (Figure 2a). The interfacial capacitance decreases with time, consistent with the adsorption of surfactants onto the gold surface to form admicelles. On the basis of these high capacitance values, the surfactant does not form an ordered monolayer film but, rather, may form linear hemicylindrical aggregates as shown by Jaschke et al.¹⁷ for sodium dodecyl sulfate (SDS) on gold. Upon addition of C₁₂SH (1 mM in 10 mM C₁₂E₆), the capacitance initially

(25) Prak, D. J.; Abriola, L. M.; Weber, W. J.; Bocskay, K. A.; Pennell, K. D. *Environ. Sci. Technol.* **2000**, *34*, 476–482.

(26) Honda, C.; Itagaki, M.; Takeda, R.; Endo, K. *Langmuir* **2002**, *18*, 1999–2003.

(27) As a relative measure of hydrophobicity, the octanol–water partition coefficient (K_{ow}) is higher for long-chain alkanethiols than for pyrene: $\log K_{ow}(\text{pyrene}) = 5.0\text{--}5.2$ (see Doong, R. A.; Chang, S. M. *Anal. Chem.* **2000**, *72*, 3647–3652) whereas $\log K_{ow}(\text{C}_n\text{SH}) = 5.5, 6.6, 8.8$, and 9.8 for $n = 10, 12, 16$, and 18 , respectively.⁴⁷

(28) Bard, A. J.; Faulkner, L. R. In *Electrochemical Methods: Fundamentals and Applications*; Wiley: New York, 1980.

(29) We chose NaF as a supporting electrolyte due to the weak interaction between the fluoride ion and gold (see Dickinson, K. M.; et al. *Electrochim. Acta* **1992**, *37*, 139–141) that should not inhibit formation of the SAM.

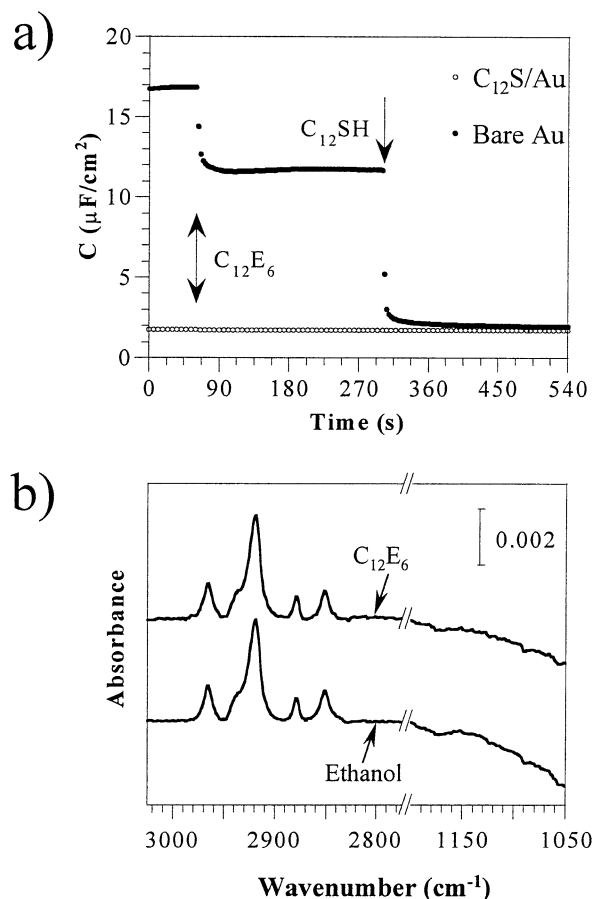


Figure 2. (a) Time dependence of interfacial capacitance for a gold electrode (closed circles) in 50 mM NaF(aq) before and after a step change in C_{12}E_6 concentration from 0 to 10 mM (maintaining constant NaF concentration), followed by a step change in C_{12}SH concentration from 0 to 1 mM (maintaining constant C_{12}E_6 and NaF concentrations). Time dependence of interfacial capacitance for a C_{12}S -coated gold electrode (open circles) before and after a step change in C_{12}E_6 concentration from 0 to 10 mM. The double-headed arrow indicates the time when C_{12}E_6 was added in each experiment, while the single-headed arrow indicates the time when C_{12}SH was added. (b) Reflectance-absorption infrared spectra for SAMs prepared by a 15 min exposure to C_{16}SH in either ethanol or 10 mM $\text{C}_{12}\text{E}_6(\text{aq})$.

decreases rapidly with time as thiols adsorb to the gold surface, forming a more densely packed film with a lower dielectric constant, and then decreases relatively slowly as the population of available surface sites diminishes. The capacitance ultimately reaches $\sim 1.9 \mu\text{F}/\text{cm}^2$, which is similar to measured ex situ values of $1.8 \mu\text{F}/\text{cm}^2$ obtained for C_{12} SAMs formed on gold in $\text{C}_{12}\text{E}_6(\text{aq})$. The rapid decrease in capacitance upon addition of C_{12}SH suggests that thiol molecules displace the surfactant molecules as the SAM is formed.

While capacitance measurements alone cannot distinguish between alkanethiolates and intercalated surfactants within the growing domains, we assert that surfactant intercalation is minimal. This proposed displacement of the admicelles by the alkanethiols is supported by ex situ contact angle measurements that show statistically no difference in SAMs prepared in $\text{C}_{12}\text{E}_6(\text{aq})$ and those prepared in ethanol (Table 3). If surfactant molecules contaminated the SAM even at as little as $\sim 1\%$ coverage, protruding ethylene oxide chains would likely affect the contact angle of water on the surface and would certainly reduce the contact angle of hexadecane, which is extremely

Table 3. Static Wetting Properties of Water and Hexadecane on $\text{C}_{16}\text{S}/\text{Au}$ SAMs^a

solvent	contact angles (advancing, receding; in deg)	
	H_2O	HD
10 mM $\text{C}_{12}\text{E}_6(\text{aq})$	118, 106	49, 37
10 mM $\text{C}_{12}\text{E}_7(\text{aq})$	117, 105	49, 37
ethanol	115, 104	48, 37

^a SAMs formed for 100 h adsorption using 1 mM C_{16}SH .

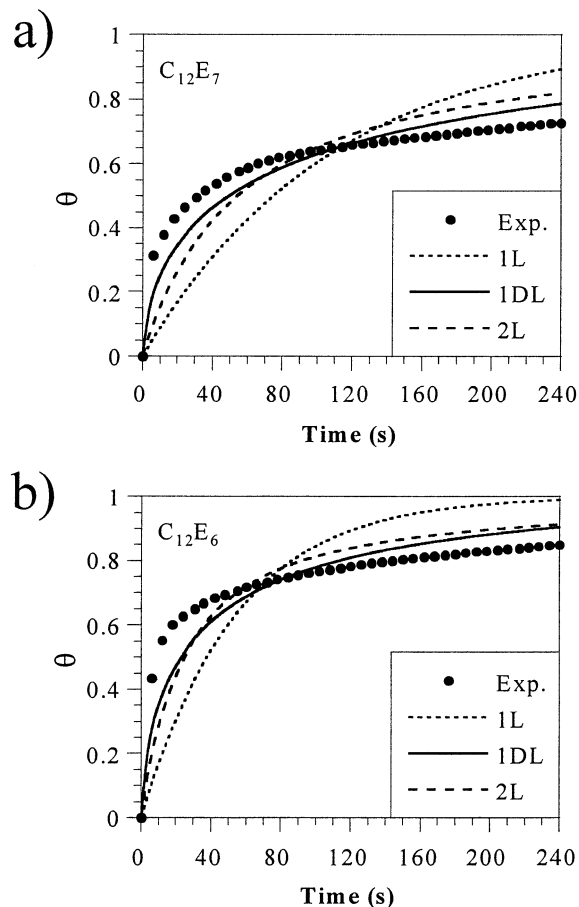


Figure 3. Time dependence of surface coverage (closed circles) upon exposure of gold to C_{16}SH in aqueous solutions containing 50 mM NaF and (a) 10 mM C_{12}E_7 or (b) 10 mM C_{12}E_6 . Enough C_{16}SH was added to form a 1 mM solution, but the actual solubilized concentration of C_{16}SH was 0.25 mM in $\text{C}_{12}\text{E}_7(\text{aq})$ and 1.0 mM in $\text{C}_{12}\text{E}_6(\text{aq})$. The curves represent model fits for first-order Langmuir (1L), first-order diffusion-limited Langmuir (1DL), and second-order Langmuir (2L) models.

sensitive to the composition at the outer $\sim 3 \text{ \AA}$ of the film.³⁰ The similarities in water and hexadecane contact angles for SAMs formed from $\text{C}_{12}\text{E}_7(\text{aq})$ and those formed in ethanol suggest no measurable incorporation of surfactant into the SAMs. These observations are further supported by ex situ infrared spectra of the formed monolayers (Figure 2b) that show no difference for SAMs formed in $\text{C}_{12}\text{E}_6(\text{aq})$ or ethanol in the range of 1100–1150 cm^{-1} where bands for the ether stretch of the ethylene oxide chains of C_{12}E_6 should appear. The absence of a signal for the ether stretch and the high-quality structures for SAMs prepared in $\text{C}_{12}\text{E}_6(\text{aq})$ ⁶ both suggest that the surfactant does not contaminate the SAM.

The use of eq 3 to monitor kinetics also assumes that the presence of a surfactant layer atop the growing SAM

(30) Laibinis, P. E.; Bain, C. D.; Nuzzo, R. G.; Whitesides, G. M. *J. Phys. Chem.* **1995**, *99*, 7663–7676.

does not contribute significantly to the measured capacitance. As shown in Figure 2a, the interfacial capacitance of a preformed C₁₂S/Au electrode does not significantly change upon introducing C₁₂E₆ into the electrolyte. While C₁₂E₆ and other surfactants are known to adsorb onto hydrophobic surfaces,³¹ this surfactant layer does not appreciably alter the interfacial capacitance from that of a high-quality SAM. The surfactant layer can be modeled as a capacitor in series with that of the SAM, and its inability to significantly alter the total interfacial capacitance suggests that it has a much higher capacitance than the SAM does. These results provide evidence to support the parallel capacitance model shown in Figure 1.

Adsorption Kinetics Models. Figure 3 shows experimental coverage data and different model fits for the adsorption kinetics of C₁₆SH onto gold in either (a) 10 mM C₁₂E₆(aq) or (b) 10 mM C₁₂E₇(aq). The coverage data are computed from in situ capacitance data using eq 3. The model fits shown in Figure 3 represent various kinetics models that have been used to describe the formation of SAMs in organic solvents:

(i) First-order, Langmuir (1L) model¹¹

$$d\theta/dt = k_{1L}c(1 - \theta) \quad (4)$$

and

$$\theta(t) = 1 - e^{-k_{1L}ct} \quad (5)$$

(ii) First-order, diffusion-limited Langmuir (1DL) model^{11,13}

$$d\theta/dt = k_{1DL}c(1 - \theta)t^{-0.5} \quad (6)$$

and

$$\theta(t) = 1 - e^{-2k_{1DL}ct^{0.5}} \quad (7)$$

(iii) Second-order, Langmuir (2L) model^{11,13}

$$\frac{d\theta}{dt} = k_{2L}c(1 - \theta)^2 \quad (8)$$

and

$$\theta(t) = \frac{k_{2L}ct}{1 + k_{2L}ct} \quad (9)$$

These models all yield grossly unsatisfactory fits to the experimental data with the first-order, diffusion-limited model providing the best fit of the three. The inability of these commonly used models to accurately fit the kinetics data suggests the kinetic process of SAM formation in aqueous micellar solutions is significantly more complex than that in organic solvents. The source of this additional complexity may be the delivery and release processes that are unique to micelle-facilitated assembly.

Development of a Model for Micelle-Assisted SAM Formation. To provide a more physically realistic description of micelle-assisted SAM formation, we have developed a model that assumes a mechanism consisting of the following steps: (1) diffusion of thiol-laden micelles from the bulk solution to the proximity of the gold surface; (2) release of the alkanethiols from the micelle, most likely to admicelles at the gold surface (vide infra); and (3)

adsorption of the alkanethiols at the metal surface after displacement of admicelles and adsorbed surfactants. The solubilization of the alkanethiols is neglected here, since the thiols are solubilized before they are added into the kinetics cell. Since the micellar carriers are dilute and their diffusion is slow relative to that of individual molecules, we assume the delivery process is slow in comparison to the release of the alkanethiols and subsequent adsorption of the thiols to the gold surface (diffusion-limited process). Each of these steps is delineated below.

Micellar Delivery. Micelles solubilize alkanethiols and function as vehicles to deliver the thiols to the proximity of the metal surface. This step can be described by the diffusion of the fully thiol-laden micelles (effective micelles) from the bulk solution to the metal surface as a semi-infinite diffusion problem. The partial differential equation for one-dimensional diffusion can be written as^{32,33}

$$\frac{\partial c_m}{\partial t} = D \frac{\partial^2 c_m}{\partial z^2} \quad (10)$$

subject to the initial and boundary conditions:

$$\text{I.C.: } c_m(z) = c_{m0} \text{ at } t = 0 \quad (11)$$

$$\text{B.C.1: } c_m(t) = 0 \text{ at } z = 0 \quad (12)$$

$$\text{B.C.2: } c_m(t) = c_{m0} \text{ at } z \rightarrow \infty \quad (13)$$

In the above equations, D is the diffusion coefficient of micelles (assumed constant) and c_{m0} is the bulk concentration of effective micelles. We assume a rapid release of alkanethiols near the metal surface so that the micelles become depleted as they reach the interface. Thus, the concentration of effective micelles near the interface is assumed to be zero during the initial stage of monolayer formation that is most sensitively probed by capacitance measurements.³⁴ The solution to eq 10 is

$$c_m = c_{m0} \operatorname{erf}\left(\frac{z}{(4Dt)^{1/2}}\right) \quad (14)$$

where $\operatorname{erf}(u)$ is the error function as $\operatorname{erf}(u) = 2/\pi^{1/2} \int_0^u e^{-y^2} dy$. The flux of effective micelles at the interface is given by

$$J_m = -D \left(\frac{\partial c_m}{\partial z} \right)_{z=0} = c_{m0} \left(\frac{D}{\pi} \right)^{0.5} t^{-0.5} \quad (15)$$

Release of Alkanethiols from Micelles. Consistent with an equilibrium between solutes in micelles and those in admicelles as inferred from adsolubilization studies,¹⁹ the alkanethiol molecules are likely released from the micelles to admicelles through a dynamic equilibrium process. In the release process, the alkanethiol must break intermolecular interactions with surfactant molecules and other solubilized thiols before transferring from the micelles into admicelles. The probability (q) of a thiol molecule leaving the micelle during a collision can be expressed in a similar manner as the probability of a

(32) Guzman, R. Z.; Carbonell, R. G.; Kilpatrick, P. K. *J. Colloid Interface Sci.* **1986**, *114*, 536–547.

(33) Crank, J. In *Mathematics of Diffusion*, 2nd ed.; Clarendon Press: Oxford, 1975.

(34) The concentration of effective micelles near the interface is not likely zero for long times after the adsorption has begun due to a decreasing adsorption rate of alkanethiols as surface sites become occupied (refer to eq 18).

(31) Ward, R. N.; Duffy, D. C.; Davies, P. B.; Bain, C. D. *J. Phys. Chem.* **1994**, *98*, 8536–8542.

surfactant dissociating from a micelle and would scale as^{35,36}

$$q = \exp\left(-\frac{E}{\kappa T}\right) \quad (16)$$

where E is the activation energy of the release process, κ is Boltzmann constant, and T is absolute temperature. Thus, the flux of thiol molecules to the metal surface becomes

$$J_A = q\sigma J_m N_{SH} = q\sigma c_{m0} N_{SH} \left(\frac{D}{\pi}\right)^{0.5} t^{-0.5} = \exp\left(-\frac{E}{\kappa T}\right) \left(\frac{D}{\pi}\right)^{0.5} \sigma c t^{-0.5} \quad (17)$$

where σ is the fractional probability of a micelle–admicelle collision, N_{SH} is the average number of solubilized alkanethiols per micelle, and c is the concentration of solubilized alkanethiols. This flux should also depend on the fractional coverage of admicelles, which is essentially unity throughout the assembly process due to the presence of admicelles on the gold surface, as well as atop the low-surface-energy domains of alkanethiolates.

Adsorption at the Surface. Upon release from the micelles to the admicelles, the alkanethiols must displace adsorbed surfactants before irreversibly adsorbing at the surface. The rate of adsorption is scaled by the coverage of available surface sites ($1 - \theta$), those not containing chemisorbed alkanethiolates. We assume an x th-order adsorption process,³⁷

$$d\Gamma/dt = J_A(1 - \theta)^x \quad (18)$$

where Γ is the adsorbance on the metal surface, and

$$\Gamma = \Gamma_\infty \theta \quad (19)$$

where Γ_∞ is the maximum adsorbance at saturated coverage. For a first-order process ($x = 1$), the adsorption rate is proportional to the number of available sites. An example of a second-order process ($x = 2$) would be a case in which displacement of the surfactant depends on both the concentration of physisorbed alkanethiol within the surface micelles and the concentration of adsorbed surfactant, both of which scale as $(1 - \theta)$. Thus, the rate would scale as $(1 - \theta)^2$.

Substituting eq 17 and eq 19 into eq 18, we obtain

$$\frac{d\theta}{dt} = \frac{\sigma}{\Gamma_\infty} \exp\left(-\frac{E}{\kappa T}\right) \left(\frac{D}{\pi}\right)^{0.5} c(1 - \theta)^x t^{-0.5} = kc(1 - \theta)^x t^{-0.5} \quad (20)$$

where k is the rate constant expressed as³⁸

$$k = \frac{\sigma}{\Gamma_\infty} \left(\frac{D}{\pi}\right)^{0.5} \exp\left(-\frac{E}{\kappa T}\right) \quad (21)$$

For a first-order adsorption ($x = 1$), integration of eq 20 gives

$$\theta = 1 - e^{-2kct^{0.5}} \quad (22)$$

which is identical in form to eq 7, although the rate constant (k) defined here has specific physical meaning

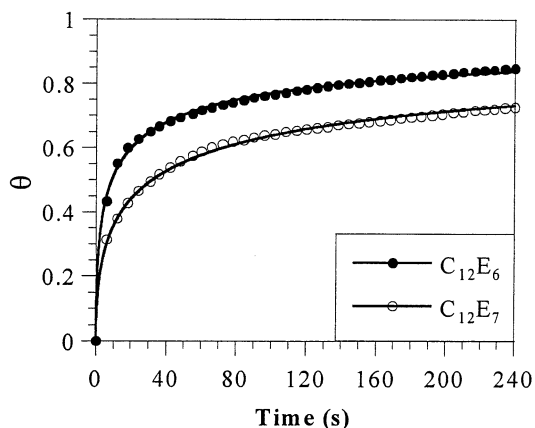


Figure 4. Time dependence of surface coverage upon exposure of gold to 1 mM $C_{16}SH$ in aqueous solutions containing 50 mM NaF and either 10 mM $C_{12}E_6$ (closed circles) or 10 mM $C_{12}E_7$ (open circles). Enough $C_{16}SH$ was added to form a 1 mM solution, but the actual solubilized concentration of $C_{16}SH$ was 0.25 mM in $C_{12}E_7(aq)$ and 1.0 mM in $C_{12}E_6(aq)$. The curves represent model fits for a diffusion-release, second-order Langmuir adsorption model (eq 23) containing a single fitted parameter k .

for a diffusion-release process. For a second-order adsorption ($x = 2$), integration of eq 20 gives

$$\theta = \frac{2kct^{0.5}}{1 + 2kct^{0.5}} \quad (23)$$

We have used a second-order diffusion-release model (23) to fit experimental coverage versus time data for the adsorption of $C_{16}SH$ (1 mM) onto gold in 10 mM aqueous solutions of $C_{12}E_6$ and $C_{12}E_7$ (Figure 4). The model provides a vastly improved agreement with the experimental kinetics data in comparison with other models (Figure 3), representing both the initial rapid increase in coverage and the slow growth of the film with time.³⁸ The high-quality fits of the experimental results by this model provide support that SAM formation in $C_{12}E_7(aq)$ is diffusion-limited, in contrast to that in organic solvents.¹¹ The fact that a second-order, diffusion-release model provides higher quality fits than a first-order model is consistent with a process in which the displacement of adsorbed surfactants is effected through associative interactions with physisorbed alkanethiols.

Effect of Micellar Concentration. The concentration of added surfactant should affect the concentration of solubilized alkanethiol and, thereby, the rate of forming the SAM. Figure 5a shows the experimental results of coverage versus time upon exposure of gold to aqueous solutions containing $C_{12}E_6$ at different concentrations and enough $C_{12}SH$ to produce a 1 mM solution if all the thiol is solubilized. The solid lines in Figure 5a represent theoretical fits based on a second-order, diffusion-release Langmuir adsorption model (23). In the range of 1–10 mM, an increase in $C_{12}E_6$ concentration corresponds to a

(37) Equation 18 is similar to that used by Rahn and Hallock (see *Langmuir* **1995**, *11*, 650–654). We have added the exponent x to allow for a more complex dependence of coverage on rate.

(38) The use of eq 21 in conjunction with either eq 22 or 23 represents a single-parameter model for describing the kinetics of SAM formation from alkanethiol-containing aqueous micellar solutions. We also developed a model that contains rate constants for both release and adsorption (two-parameter model). While the two-parameter model did provide satisfactory fits to the coverage data (perhaps due to the presence of a second adjustable parameter), the resulting rate constants determined from this fitting were physically unrealistic. The single-parameter model used herein represents a good approximation of the kinetics for the diffusion-limited case.

(35) Israelachvili, J. In *Intermolecular & Surface Forces*, 2nd ed.; Academic Press: San Diego, 1992.

(36) Aniansson, E. A. G.; Wall, S. N.; Almgren, M.; Hoffmann, H.; Kielmann, I.; Ulbricht, W.; Zana, R.; Lang, J.; Tondre, C. *J. Phys. Chem.* **1976**, *80*, 905–922.

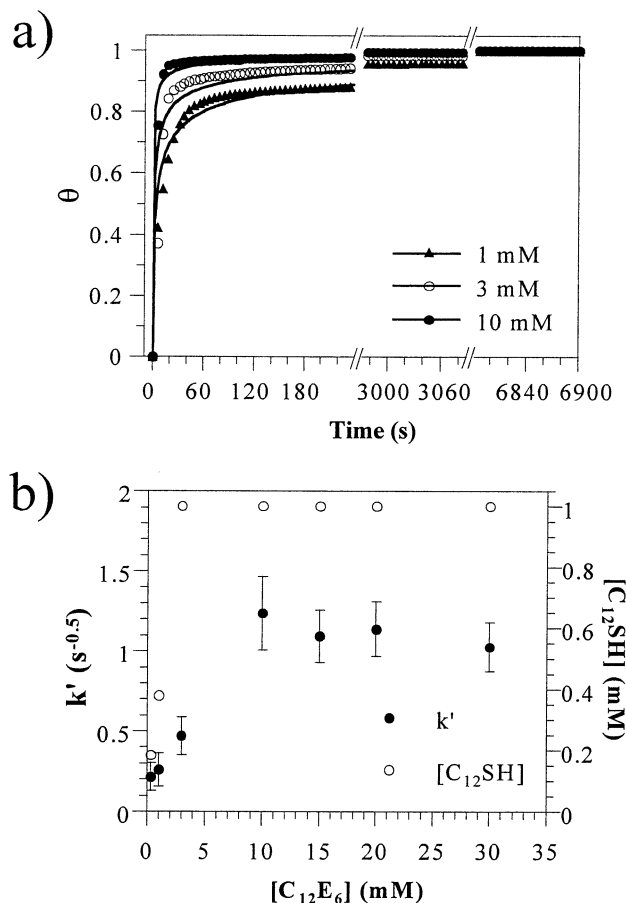


Figure 5. Effect of $C_{12}E_6$ concentration on the kinetics of formation for $C_{12}SH$ on gold. Enough $C_{12}SH$ was added to form a 1 mM solution if all the thiol is solubilized. (a) Time dependence of surface coverage at different concentrations of $C_{12}E_6$. The curves represent best fits of the data sets by a diffusion-release, second-order Langmuir adsorption model (eq 23) containing a single fitted parameter k . (b) Concentration-dependent rate constant k' (left axis, closed circles) and concentration of solubilized $C_{12}SH$ (right axis, open circles) as a function of the concentration of $C_{12}E_6$. The error bars represent standard deviations obtained after running at least three independent experiments.

more rapid increase in coverage. The effects of $C_{12}E_6$ concentration on the measured second-order, diffusion-release Langmuir rate constant ($k' = kc$) and the concentration of solubilized $C_{12}SH$ are shown in Figure 5b. At low $C_{12}E_6$ concentration, the kinetic rate increases with surfactant concentration as the higher concentration of micelles enhances the solubilization of the thiol adsorbate. At higher $C_{12}E_6$ concentration (≥ 10 mM) when all the $C_{12}SH$ is solubilized, the rate becomes constant, insensitive to the further addition of $C_{12}E_6$. The insensitivity of the rate constant at higher $C_{12}E_6$ concentration is different than that observed by Liu and Kaifer¹⁶ for monolayer formation in nonionic Triton X-100(aq). They observed the kinetic rate of SAM formation to decrease at higher surfactant concentration, presumably due to an increasing number of empty micelles (micelles without thiol molecules). These empty micelles do not contribute to the transfer of thiol molecules to the metal surface and may impede the diffusion of micelles that contain thiols, thereby reducing the kinetic rate of SAM formation. In contrast to SAM formation in Triton X-100, there are likely no empty $C_{12}E_6$ micelles in the surfactant concentration range of 3–30 mM.³⁹ The absence of empty micelles in $C_{12}E_6$ (aq) results in a rate of SAM formation that is independent of

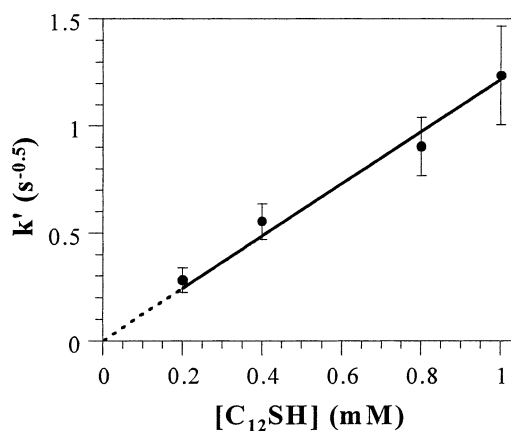


Figure 6. Effect of $C_{12}SH$ concentration on the measured rate constant for SAM formation in 10 mM $C_{12}E_6$ (aq). The line is a best fit to the data, constrained to intersect the origin. The error bars represent standard deviations obtained after running at least three independent experiments.

surfactant concentration in the range of 10–30 mM. While all (1 mM) the $C_{12}SH$ is solubilized in 3 mM $C_{12}E_6$ (aq), the slower rate at this concentration is likely due to slower diffusion of larger thiol-swollen micelles, since a typical micelle would contain an average of ~ 100 alkanethiols.

Effect of Alkanethiol Concentration. Figure 6 shows the effect of $C_{12}SH$ concentration on the measured second-order, diffusion-limited rate constant ($k' = kc$) for SAM formation in 10 mM $C_{12}E_6$ (aq). The measured rate constant increases linearly with thiol concentration, indicating that the overall rate is approximately first-order in alkanethiol concentration and thereby consistent with eq 20. These results reveal that the rate of SAM formation in $C_{12}E_6$ (aq) can be controlled in a straightforward manner by simply varying the alkanethiol concentration, perhaps more easily than in organic solvents where rate is nearly independent of alkanethiol concentration in the 0.01–1 mM range.¹³ The good linearity in Figure 6 also suggests that factors influencing the rate constant (k), namely, the micellar diffusivity (D) and the activation energy for alkanethiol release (E) (see eq 21), are not strongly affected by the surfactant to alkanethiol concentration ratio so that k is approximately independent of alkanethiol concentration.

Effect of Alkanethiol Chain Length. To gain more fundamental insight on the mechanism of micelle-assisted SAM formation, we have studied the effect of alkanethiol chain length on the kinetics of the assembly process. Figure 7a shows the coverage versus time in 1 mM C_nSH ($n = 10, 12, 16$, and 18) and 10 mM $C_{12}E_6$ (aq). As shown in Table 2, each of these thiols is completely solubilized at 1 mM concentration except for $C_{18}SH$, which is solubilized at 0.25 mM in 10 mM $C_{12}E_6$ (aq) solution. Figure 7a shows that the kinetics of SAM formation in $C_{12}E_6$ (aq) is dramatically affected by the thiol chain length and that data for all chain lengths are reasonably fit by a second-order, diffusion-release Langmuir adsorption model. Figure 7b shows the effect of alkanethiol chain length on the concentration-independent rate constant (k) for SAM formation in 10 mM aqueous solutions of $C_{12}E_6$ and $C_{12}E_7$. The concentration-independent rate constant decreases exponentially with increasing chain length of the alkanethiol in $C_{12}E_6$ (aq) and $C_{12}E_7$ (aq).¹¹ The exponential chain

(39) At the highest $C_{12}E_6$ concentration studied (30 mM), and given a 1 mM alkanethiol concentration, the micelles contain an average of ~ 10 alkanethiols. This average is based on the assumption that the aggregation number of the micelles is identical to that in the absence of thiols as reported in Table 1.

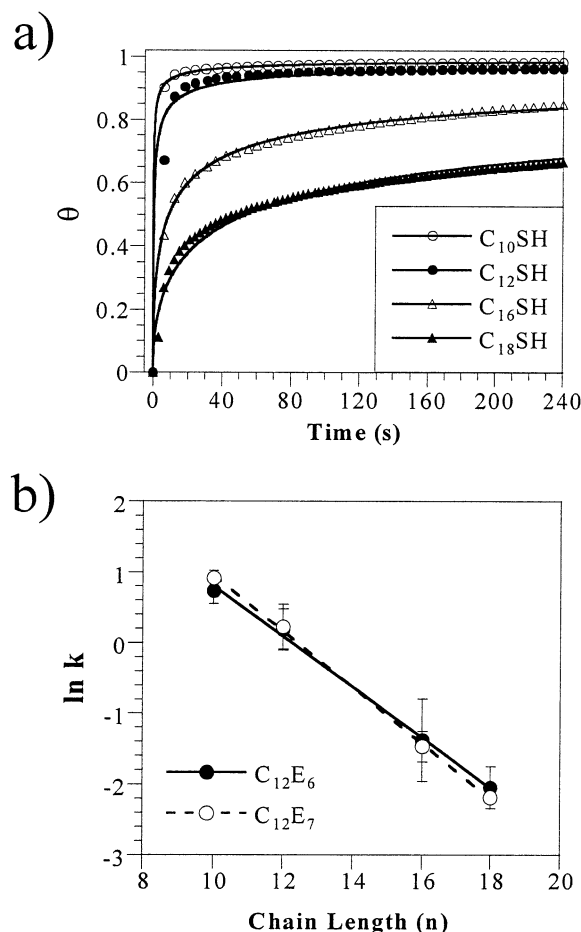


Figure 7. (a) Effect of alkanethiol chain length (n) on the kinetics of formation for $C_n\text{SH}$ on gold in 10 mM $C_{12}\text{E}_6(\text{aq})$. Enough $C_n\text{SH}$ was added to form a 1 mM solution if all the thiol is solubilized; the actual solubilized concentrations are shown in Table 2. The curves represent best fits of the data set by a diffusion-release, second-order Langmuir adsorption model (eq 23) containing a single fitted parameter k . (b) Concentration-independent, diffusion-release, second-order Langmuir rate constant k ($\text{m}^3/(\text{mol}\cdot\text{s}^{0.5})$) as a function of chain length (n) of the alkanethiol in 10 mM $C_{12}\text{E}_6(\text{aq})$ and 10 mM $C_{12}\text{E}_7(\text{aq})$ at 22 °C. The lines are best fits to the data. The slopes of the lines correspond to activation energies (ϵ_{CH_2}) of 0.21 and 0.23 kcal/mol per CH_2 group in the alkanethiol for $C_{12}\text{E}_6(\text{aq})$ and $C_{12}\text{E}_7(\text{aq})$, respectively. The error bars represent standard deviations obtained after running at least four independent experiments.

length trend for SAM formation in $C_{12}\text{E}_6(\text{aq})$ and $C_{12}\text{E}_7(\text{aq})$ is consistent with a larger activation energy for release of longer-chained thiols compared to shorter-chained analogues. The activation energy increases linearly with the number of methylene units⁴⁰ and can be expressed as

$$E = (n - 1)\epsilon_{\text{CH}_2} + \epsilon_{\text{CH}_3} + \epsilon_{\text{SH}} \quad (24)$$

where ϵ_{CH_2} is the activation energy per CH_2 group and $\epsilon_{\text{CH}_3} + \epsilon_{\text{SH}}$ is the sum of the activation energies contributed from the CH_3 and SH groups. From eq 21 and eq 24, we obtain

$$\ln k = \ln\left(\frac{\sigma D^{0.5}}{\Gamma_{\infty} \pi^{0.5}}\right) - \frac{\epsilon_{\text{CH}_3} + \epsilon_{\text{SH}}}{kT} - \frac{\epsilon_{\text{CH}_2}}{kT}(n - 1) \quad (25)$$

where the last term on the right-hand side provides the dominant dependence on the chain length of the alkanethiol. On the basis of the slopes of the data sets in Figure 7b, the activation energy (ϵ_{CH_2}) for release of the thiols

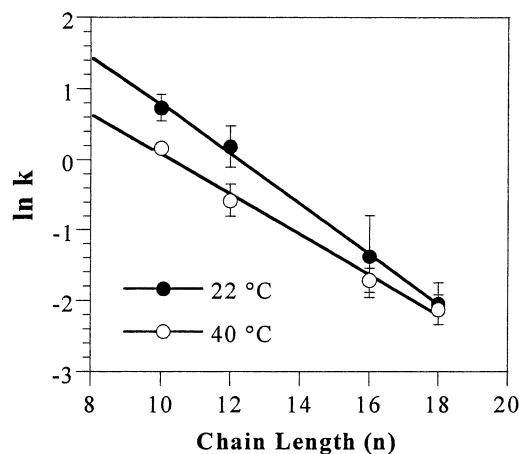


Figure 8. Effect of alkanethiol chain length on the second-order, diffusion release rate constant k ($\text{m}^3/(\text{mol}\cdot\text{s}^{0.5})$) for SAM formation on gold in 10 mM $C_{12}\text{E}_6(\text{aq})$ at 22 and 40 °C. The lines are best fits to the data. The slopes of the lines correspond to activation energies (ϵ_{CH_2}) of 0.21 and 0.18 kcal/mol per CH_2 group in the alkanethiol at 22 and 40 °C, respectively. The error bars represent standard deviations obtained after running at least three independent experiments. When no error bar is present, the error is approximated by the size of the symbol.

from the micelle increases by 0.21 and 0.23 kcal/mol per CH_2 unit in the alkanethiol in $C_{12}\text{E}_6(\text{aq})$ and $C_{12}\text{E}_7(\text{aq})$, respectively. This increase of activation energy with thiol chain length is significantly less than that of ~ 0.7 kcal/mol per CH_2 unit for the dissociation of a variety of alkyl surfactants from micelles to water^{36,41} and for partitioning of alkanes from micelles to water.^{25,42}

The similarity in rates of formation for SAMs in $C_{12}\text{E}_6(\text{aq})$ and $C_{12}\text{E}_7(\text{aq})$ suggests that the principal micellar vehicles in these two systems exhibit similar diffusivities and are, therefore, of similar shape and size. To our knowledge, there has been no investigation on the size and structure of $C_{12}\text{E}_6$ and $C_{12}\text{E}_7$ micelles with added oil-like molecules. On the basis of studies of dilute solutions of pure micelles (no additives) in water as shown in Table 1, $C_{12}\text{E}_6$ forms a mixture of spherical and cylindrical micelles at room temperature⁸ while $C_{12}\text{E}_7$ forms primarily spherical ones.⁹ Kato et al.⁴³ have shown that a 2.2 mM solution of $C_{12}\text{E}_6(\text{aq})$ at 25 °C contains mostly spheroidal micelles with aggregation numbers near 115 with a smaller fraction of larger micelles with high aggregation numbers. The presence of these larger cylindrical micelles in $C_{12}\text{E}_6(\text{aq})$ likely explains the higher solubility of long-chain alkanethiols in $C_{12}\text{E}_6(\text{aq})$ versus $C_{12}\text{E}_7(\text{aq})$. However, since the smaller spheroidal micelles greatly outnumber the larger cylindrical ones in $C_{12}\text{E}_6(\text{aq})$ at room temperature, we would then expect these faster diffusing spheroidal micelles to provide the dominant contribution toward the delivery of alkanethiols to the gold surface. The similarity of these dominant carrier micelles in $C_{12}\text{E}_6(\text{aq})$ and $C_{12}\text{E}_7(\text{aq})$ likely explains the similar rates of SAM formation in these systems (Figure 7b).

We also examined the rates of SAM formation in 10 mM $C_{12}\text{E}_6(\text{aq})$ at 40 °C (Figure 8), a temperature at which the micelles are polydisperse and wormlike, exhibiting much higher aggregation numbers than those obtained at room temperature.⁸ The rates of assembly for $C_{10}\text{SH}$

(40) Tanford, C. In *The Hydrophobic Effect*; Wiley-Interscience: New York, 1973, and references therein.

(41) Bolt, J. D.; Turro, N. J. *J. Phys. Chem.* **1981**, *85*, 4029–4033.
(42) Woodrow, B. N.; Dorsey, J. G. *Environ. Sci. Technol.* **1997**, *31*, 2812–2820.

(43) Kato, T.; Kanada, M.-A.; Seimiya, T. *J. Colloid Interface Sci.* **1996**, *181*, 149–158.

and $C_{12}SH$ in $C_{12}E_6(aq)$ are significantly faster at room temperature than at 40 °C. The slower formation at 40 °C is consistent with slower diffusion of the larger wormlike micelles. On the basis of the intercept of the two lines in Figure 8, the ratio of the micelle diffusion coefficients at 22 and 40 °C is $\sim 14:1$. The smaller slope for the data set at 40 °C corresponds to an activation energy of 0.18 kcal/mol per CH_2 group, indicating a smaller barrier for release of the alkanethiols from the larger micelles at higher temperatures. This finding is consistent with the enhanced rates of surfactant dissociation³⁶ and solute transfer⁴⁴ from micelles at higher temperatures.

Discussion

The formation of SAMs in aqueous micellar solutions is more complex than that in traditional organic solvents. For alkanethiolate SAM formation in organic solvents, the kinetic rate of formation generally decreases with increasing thiol chain length (n), but not exponentially.¹¹ The rate-limiting step in organic-solvent-borne processes has been attributed to displacement of solvent molecules from the surface. In such a process, the rate of formation depends on the mobility of the adsorbate, which theoretically scales as $1/n$.⁴⁵ In agreement with theory, Dannenberger et al.¹¹ achieved satisfactory linearity when plotting the observed experimental rates of SAM formation from hexane versus $1/n$.

In $C_{12}E_6(aq)$ and $C_{12}E_7(aq)$, the exponential dependence of the rate constant on alkanethiol chain length and the high-quality fits of the kinetics data to a diffusion-limited model suggest an inherently more complex process than that in solvent-borne assembly. The results described in the previous section reveal several important clues regarding the mechanism of micelle-assisted SAM formation: (1) alkanethiols displace the adsorbed surfactants from the surface and form a densely packed monolayer film; (2) the kinetics results are consistent with a second-order, diffusion-limited process and are not fit by simpler models that effectively describe SAM formation from organic solvents; (3) the rate of forming the SAM depends strongly on the concentration of solubilized alkanethiol; (4) the rate decreases exponentially with increasing alkanethiol chain length, exhibiting a fairly small activation energy for release of the thiols from the micelles to the metal surface; (5) temperature is known to alter the size of the micellar carriers,⁴⁶ which, in turn, affects their diffusivity and the rate of SAM formation. These results are consistent with a mechanism in which the micellar vehicles deliver the alkanethiols near the gold surface to form the monolayer. The diffusion limitation of this process indicates that the delivery process is slow compared to the subsequent events required to incorporate the alkanethiols into the growing SAM. Nonetheless, the exponential chain length dependence of this process suggests that release of the alkanethiols from the micelle, which defines the concentration of active alkanethiols at or near the surface, is an important aspect of the overall assembly process. The mechanistic details of this release process, including the likely role of $C_{12}E_j$ admicelles, are discussed in detail below.

One explanation for the observed exponential chain length dependence of the rate constant is that the rate is affected by the solubility of free alkanethiols in water.

The solubility of free alkanethiols is indeed expected to decrease exponentially in water as chain length is increased.⁴⁷ However, such reasoning would suggest that micelles are not necessary to form alkanethiolate SAMs in aqueous solutions. In contrast, the observed rate of formation depends on the concentration of solubilized alkanethiol that is dramatically enhanced by the presence of the micelles. Another possible explanation is that the micelles boost the concentration of free alkanethiols by dispersing the thiols in solution and then allowing these thiols to partition into the aqueous phase. However, the tendency for these long-chain alkanethiols to partition from the micellar core into water is extremely low. Using an average micelle–water partition coefficient of $\sim 10^9$, which was measured for dodecane in $C_{12}E_8$ micelles,²⁵ the concentration of free alkanethiols in this study would be $\sim 10^{-9}$ mM, far too low a concentration to produce rates of formation as rapid as those observed in this work. Finally, the activation barrier of ~ 0.2 kcal/mol per CH_2 group, derived from the results of Figure 7b, is well below that expected for the release of alkanethiols from the micellar core directly into water. On the basis of the measured partitioning of alkanes from $C_{12}E_8$ micelles to water (0.72 kcal/mol per CH_2 group)^{25,42} and for surfactant dissociation from micelles (~ 0.7 kcal/mol per CH_2 group),^{36,41} the activation barrier for the micelle–water partitioning of an alkanethiol should also be approximately 0.7 kcal/mol per CH_2 group. The much smaller activation energy here suggests that these long-chain alkanethiols do not release directly into water prior to adsorption.

A more plausible model for micelle-assisted SAM formation should consider interactions between thiol-laden micelles in solution and micelles adsorbed at the gold surface. As suggested by the capacitance data in Figure 2, $C_{12}E_j$ surfactants are adsorbed at the gold surface prior to introducing the thiol-containing $C_{12}E_j$ solution. These surfactants are likely organized into admicelles (most likely long, continuous, hemicylindrical structures similar to those formed by sodium dodecyl sulfate on gold).¹⁷ These surface micelles are quite robust, as evidenced by their stability when imaged by an AFM probe. To deliver alkanethiols to the surface, thiol-laden micelles in solution must diffuse to the surface and either displace the admicelles or interact with them to enable the release of alkanethiols from the solution micelles to the admicelles. Since rapid displacement of these stable admicelles by micelles in solution is unlikely, we will focus on the release of alkanethiols between the micelles and admicelles.

On the basis of the presumed importance of micelle–admicelle interactions, another model to describe SAM formation in aqueous micellar solutions draws from micellar interactions in solution. Rharbi et al.^{44,48} have investigated the exchange of water-insoluble solutes between nonionic Triton X-100 micelles in solution through stopped-flow fluorescence time-scan measurements. They have reported that solute exchange in nonionic micellar solutions occurs primarily through a fusion–fragmentation process where a solute-laden micelle combines with an empty micelle to form one larger micelle that then fragments with redistribution of the solutes. The fusion process is independent of solute hydrophobicity. In our system, such a fusion process could hypothetically occur between thiol-rich solution micelles and thiol-lean admicelles, thereby transferring the alkanethiols to the surface for subsequent incorporation into the growing

(44) Rharbi, Y.; Winnik, M. A. *Adv. Colloid Interface Sci.* **2001**, 89–90, 25–46.

(45) de Gennes, P. G. *J. Chem. Phys.* **1971**, 55, 572–579.

(46) Puvvada, S.; Blankschtein, D. *J. Chem. Phys.* **1990**, 92, 3710–3724.

(47) Schwarzenbach, R.; Gschwend, P.; Imboden, D. In *Environmental Organic Chemistry*; Wiley: New York, 1993.

(48) Rharbi, Y.; Li, M.; Winnik, M. A.; Hahn, K. G. *J. Am. Chem. Soc.* **2000**, 122, 6242–6251.

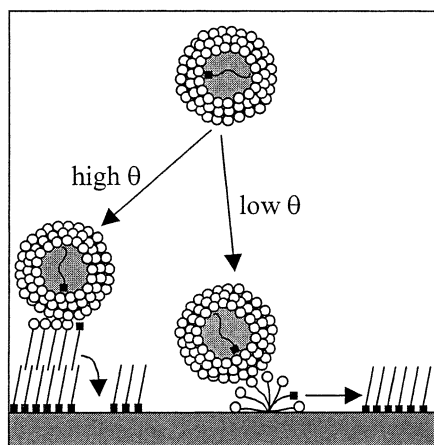


Figure 9. Proposed mechanism for the micelle-assisted formation of SAMs. At low coverage, alkanethiols are transferred from micelles to admicelles, most likely through a collision-induced, activated-diffusion process. The thiols displace adsorbed surfactants and admicelles and adsorb onto the gold surface to form oriented alkanethiolates. At high coverage, the alkanethiols must release into surfactant bilayers that are present atop the growing SAM.

SAM. Nonetheless, since a complete fusion mechanism would be independent of the solute hydrophobicity,⁴⁸ longer-chained alkanethiols would release to the surface at similar rates as shorter-chained analogues. The exponential alkanethiol chain length dependence observed for SAM formation in $C_{12}E_7(aq)$ is incompatible with such a fusion-mediated process. The enhanced confinement of the surfactants in these hemicylindrical admicelles likely hinders their capability toward complete fusion with micelles from solution.

Since a complete fusion process between micelles and admicelles is inconsistent with the kinetics results, we explored other types of interactions between micelles. Taisne and Cabane⁴⁹ have suggested that exchange of tetradecane molecules between microemulsion droplets of $C_{12}E_5$ occurs by permeation of the tetradecane through the intervening poly(ethylene oxide) region during collisions between the droplets. Similar to a fusion mechanism, this so-called "sticky collision" mechanism for solute transfer in micellar solutions is expected to depend on the solute concentration in loaded micelles and the concentration of empty micelles. While Rharbi et al.⁴⁸ have argued that this sticky collision mechanism is less likely than a fusion mechanism to explain the exchange of solutes between nonionic micelles *in solution*, the sticky collision model may be more appropriate to describe the interaction of a micelle with an admicelle where the fusion process is energetically inhibited. As applied to the micelle-assisted formation of SAMs, the sticky collision model implies that the thiol-laden micelles diffuse to the surface where they collide with admicelles. The collision would be expected to perturb the structure of the micelle, but not to the extent of a complete fusion process. As schematically shown in Figure 9, the alkanethiols in the micelle can release to the admicelle by diffusing across the polar poly(ethylene oxide) region separating the micellar and admicellar cores. This diffusion process is expected to be activated and would depend on the solubility of the alkanethiol in the micellar corona. The process is then dependent on the hydrophobicity, and thus the chain length, of the alkanethiol. The barrier associated with this process would be considerably smaller than that for release of the alkanethiol into water,

qualitatively consistent with the small energy barrier obtained from the results in Figure 7b. The barrier should become even smaller at higher temperatures due to the enhanced dehydration of the poly(ethylene oxide) chains of $C_{12}E_7$,⁴⁶ consistent with the results from Figure 8 where the activation energy at 40 °C is ~15% lower than that at 22 °C.

If the release of alkanethiols involves interaction between micelles and admicelles, the rate of SAM formation should be reduced in ionic surfactant systems due to electrostatic repulsion between the charged micelles. Rharbi et al.⁴⁴ have shown that exchange of insoluble solutes between anionic micelles in solution is dramatically slower than exchange in nonionic micellar solutions. We have observed that the rates of SAM formation in micellar solutions of the cationic surfactant dodecyltrimethylammonium bromide ($C_{12}TAB$) are reduced from those in $C_{12}E_6(aq)$ and $C_{12}E_7(aq)$.⁵⁰ In fact, SAM formation in $C_{12}TAB(aq)$ is not diffusion limited, suggesting a significantly slower process required for release and/or adsorption at the surface. We are currently preparing a manuscript to discuss the important differences between SAM formation in these cationic and nonionic micellar systems.⁵⁰

Our previous results⁶ have established that micelle-assisted SAMs are highly crystalline, densely packed films with almost no defects. The proposed mechanism (Figure 9) is also consistent with the gradual filling in of remaining surface sites by alkanethiols that is required to produce such a densely packed monolayer. At high coverages of thiolates, the admicelles are most likely present as bilayers atop the hydrophobic domains of thiolates,³¹ thereby providing a useful medium for the release of alkanethiols from solution. These thiols can ultimately adsorb from the micellar bilayer into the few remaining surface sites as the thiolate coverage approaches unity (Figure 9). A recent report by Geissler et al.⁵¹ on the etch resistance of $C_{16}S$ -SAMs formed from $C_{12}E_6(aq)$ provides evidence to support our hypothesis that alkanethiols transfer from the micellar bilayer atop well-formed regions of alkanethiolates to open sites on the gold surface.

Conclusions

In a summary, the formation of a SAM from alkanethiol-containing aqueous solutions of $C_{12}E_6$ and $C_{12}E_7$ is consistent with a series of steps in which (1) the micelles solubilize the hydrophobic alkanethiols, (2) the thiol-laden micelles diffuse near the gold surface, (3) the thiols transfer out of the micelles, most likely through a collision-induced, activated diffusion process into admicelles that are present on the gold surface or atop the growing thiolate domains, and (4) the thiols displace the adsorbed surfactant molecules, and chemisorb onto the gold surface. This proposed mechanism for the micelle-assisted formation of SAMs in nonionic micellar solutions is distinct from that in ionic micellar solutions. The results provide fundamental implications for various micellar delivery processes, especially those that involve micelle–admicelle interactions.

Experimental Section

Materials. Gold shot (99.99%) and silicon (100) wafers were obtained from J&J Materials (Neptune City, NJ) and Montco Silicon (Royersford, PA), respectively. All chemicals, including

(49) Taisne, L.; Cabane, B. *Langmuir* **1998**, *14*, 4744–4752.

(50) Yan, D.; Jordan, J. L.; Burapatana, V.; Jennings, G. K. *Langmuir*, in press.

(51) Geissler, M.; Schmid, H.; Bietsch, A.; Michel, B.; Delamarche, E. *Langmuir* **2002**, *18*, 2374–2377.

n-alkanethiols (Aldrich), poly(oxyethylene) monoalkyl ethers ($C_{12}E_6$ and $C_{12}E_7$; Fluka), sodium fluoride (Fisher), 100% ethanol (AAPER), and deuterium oxide (D_2O ; 99.9% atom D; Aldrich) were used as received. Deionized water (16.7 M Ω) was purified with a Modu-Pure system.

Sample Preparation. Gold substrates were prepared by evaporating 1000–1500 Å of gold at a rate of 1–3 Å/s onto silicon [Si(100)] wafers inside a diffusion-pumped chamber with a base pressure of 4×10^{-6} Torr. Prior to the evaporation of gold, a 100 Å layer of chromium was evaporated onto silicon to serve as a primer.

SAM Preparation for ex Situ Studies. SAMs were prepared by immersing evaporated gold films into solutions containing 1 mM $C_{16}SH$ in 10 mM $C_{12}E_6(aq)$, 10 mM $C_{12}E_7(aq)$, or ethanol at room temperature for 100 h. Upon removal, the samples were rinsed with fresh solvent ($C_{12}E_7(aq)$ or ethanol) and water and dried under a stream of nitrogen.

In Situ Monitoring of SAM Formation. Capacitance measurements were taken with a CMS300 electrochemical impedance system (Gamry Instruments) interfaced to a personal computer. Measurements were taken inside a Teflon cell containing a gold working electrode with a 1 cm² fixed area. The cell initially contained 1 mL of 50 mM NaF(aq) and the desired concentration of surfactant ($C_{12}E_j$). After a stable capacitance was obtained, a 6 mL aqueous solution of 1 mM alkanethiol, 50 mM NaF, and the desired $C_{12}E_j$ concentration was added. In this manner, 1 mM represents the maximum solution concentration of thiol in the cell if sufficient surfactant is present to solubilize the thiol. Capacitance readings were recorded every 3 or 6 s and were obtained from the imaginary impedance at 100 Hz. For SAMs formed from octadecanethiol ($C_{18}SH$), the solutions were first heated to 35 °C to melt the thiol and facilitate solubilization before cooling to room temperature for the assembly.

Reflectance–Absorption Infrared Spectroscopy. IR spectra were obtained in a single reflection mode with a Bio-Rad

Excalibur infrared spectrometer equipped with a universal reflectance attachment. The polarized light was incident at 80° from the surface normal. The reflected light was detected with a narrow-band MCT detector cooled with liquid nitrogen. Spectral resolution was 2 cm⁻¹ after triangular apodization. Spectra were referenced to those of SAMs prepared on gold from octadecanethiol-*d*₃₇, and 1000 scans of both sample and reference were collected.

Wetting Measurements. Advancing and receding contact angles were measured on static drops of water or hexadecane with a Rame-Hart manual goniometer. Contacting liquids were advanced or retreated ($\sim 1 \mu L/s$) prior to measurement via an attached syringe supplied by Rame-Hart. The syringe tip remained in the drop during measurement. Both sides of $\sim 5 \mu L$ drops were measured at two different locations on a sample.

Nuclear Magnetic Resonance. The ¹H NMR measurements were performed with a Bruker DRX 400 MHz NMR spectrometer. The spectra were recorded over 128 scans using 5 mm tubes with D_2O as a solvent. The characteristic peak for alkanethiols is that due to $-CH_2SH$ (chemical shift, 2.4) and for $C_{12}E_j$ is that due to $-(OCH_2CH_2)_n$ (chemical shift, 3.3–3.7). The characteristic peaks of alkanethiols and surfactants are clearly separated. Since the concentration of surfactant is known, the concentration of solubilized alkanethiol is determined from the ratio of the integrated areas of the characteristic peaks.

Acknowledgment. We gratefully acknowledge financial support from the NSF (CTS-9983966). We thank the Vanderbilt University School of Engineering for partial support of J.A.S. in the Summer Undergraduate Research Program.

LA020406K